



X-ray and DFT Investigation of (E)-4-bromo-5-methoxy-2-((o-tolylimino)methyl)phenol Compound

(E)-4-brom-5-metoksi-2-((o-tolilimino)metil)fenol Bileşiğinin X-ışını ve YFK ile İncelenmesi

Nur Bektaş¹ , Zeynep Demircioğlu² , Çiğdem Albayrak Kaştaş³ , Orhan Büyükgüngör¹ 

¹Ondokuz Mayıs University, Faculty of Arts and Sciences, Department of Physics, Samsun, Turkey

²Sinop University, Faculty of Arts and Science, Department of Physics, Sinop, Turkey

³Sinop University, Faculty of Arts and Science, Department of Chemistry, Sinop, Turkey

Abstract

(E)-4-bromo-5-methoxy-2-((o-tolylimino)methyl)phenol was investigated by experimental and theoretical methodologies. The solid state molecular structure was determined by X-ray diffraction method. All theoretical calculations were performed by density functional theory (DFT) method by using B3LYP/6-31G(d,p) basis set. The titled compound showed the preference of enol form, as supported by X-ray diffraction method. The geometric and molecular properties were compared for both enol-imine and keto-amine forms for title compound. Stability of the molecule arises from hyperconjugative interactions, charge delocalization and intramolecular hydrogen bond has been analyzed using natural bond orbital (NBO) analysis. Mulliken population method and natural population analysis (NPA) have been studied. Also, condensed Fukui function and relative nucleophilicity indices calculated from charges obtained with orbital charge calculation methods (NPA). Molecular electrostatic potential (MEP) and non linear optical (NLO) properties are also examined.

Keywords: Fukui function analysis, Natural bond analysis (NBO), Natural population analysis (NPA), Nonlinear optical properties (NLO), X-ray diffraction method

Öz

(E)-4-bromo-5-methoxy-2-((o-tolylimino)methyl)phenol bileşiği deneysel ve kuramsal yöntemlerle incelenmiştir. Bileşiğin moleküler yapısı X-ışını kırınım yöntemiyle aydınlatılmıştır. Tüm kuramsal hesaplamalarda Yoğunluk Fonksiyonel Kuramı (YFK) Becke tipi 3-parametrelili (B3LYP)/6-31G(d,p) baz seti ile hesaplanmıştır. X-ışını kırınımı sonuçları yapının enol-imin formda olduğunu öngörmüştür. Moleküler ve geometrik özellikler ise hem enol-imin hem de keto-amin formunda incelenmiştir. Hiperkonjuge etkisini, yük delokalizasyonu ve hidrojen bağından kaynaklı molekül kararlılığı doğal bağ analizi (NBO) ile incelenmiştir. Mulliken popülasyon analizi ve doğal popülasyon analizi hesaplanmıştır. Bunlara ilave olarak Fukui fonksiyon analizi ve yük yardımıyla nükleofilik indisler orbital yük hesaplama methodu (NPA) kullanılarak incelenmiştir. Ayrıca Moleküler Elektrostatik Potansiyel haritası (MEP) ve ikinci dereceden lineer olmayan optik özellikler (NLO) hesaplanarak tartışılmıştır.

Anahtar Kelimeler: Fukui fonksiyon analizi, Doğal bağ analizi (NBO), Doğal popülasyon analizi (NPA), Lineer olmayan optik özellikler (NLO), X-ışını kırınım yöntemi

1. Introduction

Structurally, a Schiff base (also known as imine or azomethine) is a nitrogen analogue of an aldehyde or ketone in which the carbonyl group (C=O) has been replaced by an

imine or azomethine group. o-hydroxy Schiff bases can exist in two tautomeric form as enol and keto forms in the solid state (Özek et al. 2007). Schiff bases are used as pigments and dyes, catalysts, intermediates in organic synthesis, and as polymer stabilisers. Schiff bases have also been shown to exhibit a broad range of biological activities, including antifungal, antibacterial, antimalarial, antiproliferative, anti-inflammatory, antiviral, and antipyretic properties (Dhar and Taploo 1982).

*Corresponding author: zeynep.kelesoglu@omu.edu.tr

Nur Bektaş  orcid.org/0000-0003-0427-225X

Zeynep Demircioğlu  orcid.org/0000-0001-9538-9140

Çiğdem Albayrak Kaştaş  orcid.org/0000-0003-0235-7460

Orhan Büyükgüngör  orcid.org/0000-0001-7133-1841

A new (E)-4-bromo-5-methoxy-2-((o-tolylimino)methyl) phenol compound was synthesized and it was determined by single crystal X-ray diffraction technique. MEP, NLO, Mulliken charges and NPA analysis of the titled compound by using DFT with B3LYP/6-31G(d,p) basis set. Electrophilic and nucleophilic attack and the region of chemical reactivities were also calculated by Fukui function analysis. The redistribution of electron density in various bonding and antibonding orbitals along with $E^{(2)}$ energies were calculated by natural bond orbital (NBO) using same level theory and chemical activity was also evaluated in the way of molecular orbital framework.

2. Materials and Method

2.1. Synthesis

The compound (E)-4-bromo-5-methoxy-2-[(o-tolylimino)methyl]phenol was prepared by refluxing a mixture of a solution containing 5-bromo-2-hydroxy-4-methoxybenzaldehyde (0.3 g, 1.3 mmol) in 20 mL ethanol and a solution containing 2-methylaniline (0.14 g, 1.3 mmol) in 20 mL ethanol. The reaction mixture was stirred for 2 h under re-

flux. The crystals suitable for X-ray analysis were obtained by slow evaporation from ethanol (yield: 78%).

2.2. Crystal Structure Determination and Computational Details

The single-crystal X-ray data were collected on a STOE IPDS II image plate diffractometer. The structure was solved by direct methods using SHELXS-2013 (Stoe 2002) and refined through the full-matrix least-squares method using SHELXL-2014 (Stoe 2002), implemented in the WinGX (Sheldrick 2008) program suite. The data collection conditions and parameters of refinement process are listed in Table 1. All theoretical studies of the title compound were calculated by using the DFT/B3LYP combined with standard 6-31G(d,p) basis set and GAUSSIAN 09W (Gaussian09 2009) program package without any constraint on the geometry.

3. Results

3.1. Crystal Structure and Optimized Geometry

The tautomerism appears in o-hydroxy Schiff bases shows

Table 1. Crystal data and structure refinement parameters.

Chemical formula	$C_{15}H_{14}BrN_1O_3$
Color/shape	Yellow/Plate
Formula weight	320.18
Temperature	296 K
Crystal system	Monoclinic
Space group	C2/c
Unit cell parameters	a= 25.4889(12) Å b= 7.0821(4) Å c= 16.0643(7) Å
	$\beta = 109.193(3)^\circ$
Volume	2738.64(22) Å ³
Z	8
Density	1.553 Mgm ⁻³
Absorption coefficient	3.01 mm ⁻¹
Diffractometer/meas. meth.	STOE IPDS 2 / v-scan
θ range for data collection	1.7°-26.5°
Measured reflections	8756
Independent/observed reflections	2827/2054
Goodness of fit on F^2	1.016
Final R indices [$I > 2\sigma(I)$]	R1=0.038 wR2=0.077
R indices (all data)	R1=0.063 wR2=0.085

Table 2. Hydrogen bonding geometry for the titled compound.

D-H...A	D-H	H...A	D...A	D-H...A
O1-H1...N1	0.82	1.92	2.6524(4)	148

D: donor; A: Acceptor.

two types of intramolecular hydrogen bonds as O–H...N in enol-imine form and N–H...O in keto-amine form (Figure 1). X-ray diffraction method shows that the C=N double bond and C–O single bond distances (Table 3) indicates that the compound adopts enol-imine form. The strong intramolecular interaction between the phenolic atom O1 and nitrogen atom N1 forms a six-membered ring defined as S(6) in Etter's notation (Etter, 1990). The H1 atom is located on atom O1 and constitutes the O1-H1...N1 hydrogen bonding (Figure 2, Table 2). X-ray results show the dihedral angle between the planes of two aromatic rings is 12.43(2)° and in optimized geometries are 38.65° (enol-imine form) and 8.03° (keto-amine form). In addition, the dihedral angle between the nearly planar S(6) (O1/H1/N1/C8/C1/C6) ring with C1–C6 (Cg1) and C9–C14 (Cg2) aromatic rings are 13.3(15)° and 2.94(15)°, respectively. In addition, the dihedral angle between the nearly planar S(6) (O1/H1/N1/C8/C1/C6) ring with C1–C6 (Cg1) and C9–C14 (Cg2) aromatic rings are 13.3(15)° and 2.94(15)°, respectively. The results indicated that a little differences in experimental and computational processes (Table 3). The differences observed between the experimental and calculated parameters were due to the ignored effects for gas phase. Theoretical methods were not taken into account the molecular interactions. The crystal packing of the title compound is mainly stabilized by C–H...π interactions. The r.m.s. fit of the atomic positions of experimental and calculated geometries are 0.129 Å and 0.445 Å, indicating the two geometries for enol-imine and keto-amine form, respectively (Figure 4). The theoretical results of the geometric parameters are successfully represented experimental data.

3.2. Molecular Properties from Orbital Energies (Frontier Molecular Orbitals) and Chemical Activity

The most important frontier molecular orbitals (FMOs) such as highest occupied molecular orbital (HOMO) and lowest unoccupied molecular orbital (LUMO) are very important parameters for chemical stability of the molecule (Murray and Sen 1996). The HOMO is the orbital that primarily acts as an electron donor and the LUMO is the orbital that largely acts as the electron acceptor (Boyle et al 2008). The gap between HOMO and LUMO characterizes

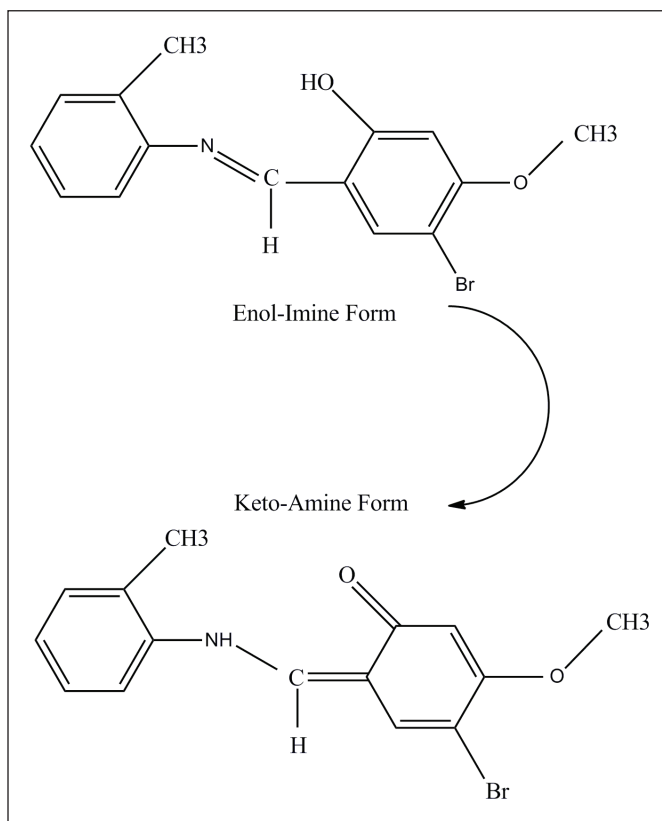


Figure 1. Enol-imine and keto-amine tautomeric forms of title compound.

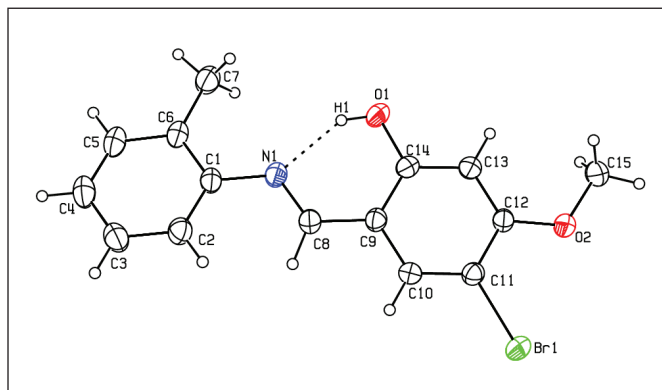
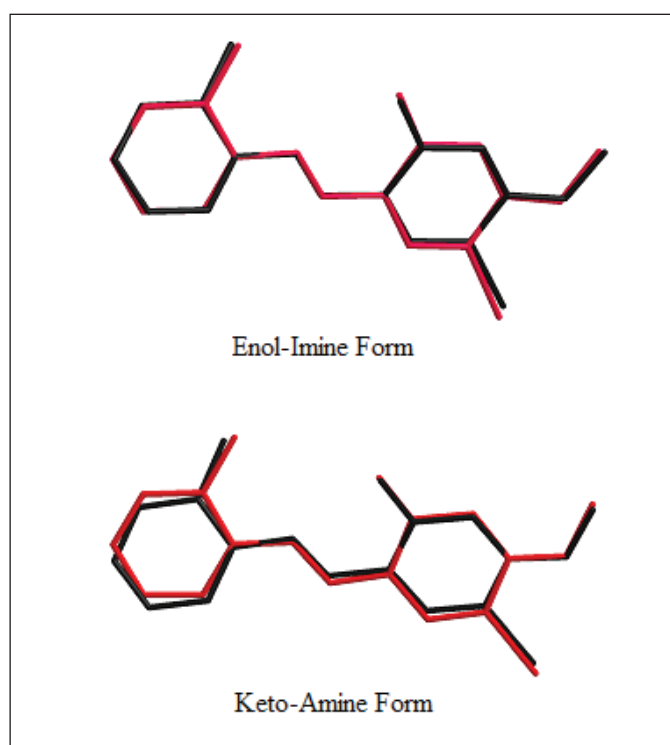


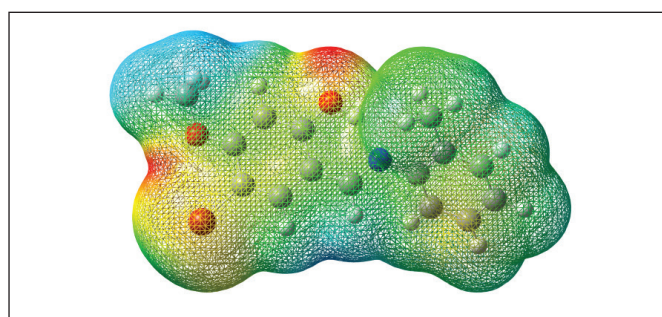
Figure 2. Ortep 3 diagram for the title compound, with the atom numbering scheme. Dashed lines are show the O1-H1...N1 intra molecular hydrogen bonds.

Table 3. Selected geometric parameters obtained by X-ray and DFT/B3LYP/6-31G(d,p).

Geometric Parameters	Experimental	DFT Enol-Imine	DFT Keto-Amine	Geometric Parameters	Experimental	DFT Enol-Imine	DFT Keto-Amine
C8-N1	1.274 (4)	1.294	1.333	N1-C8-C9	123.1 (3)	122.084	121.916
C1-N1	1.426 (4)	1.409	1.406	C9-C14-O1	121.1 (3)	121.632	121.718
C8-C9	1.445 (4)	1.444	1.396	C10-C11-Br	119.4 (2)	120.083	120.427
O1-C14	1.343 (3)	1.337	1.265	C1-N1-C8-C9	177.9 (3)	-176.744	-179.747
O2-C15	1.427 (4)	1.423	1.423	N1-C8-C9-C14	-1.2 (5)	0.224	-0.402
C11-Br	1.883 (3)	1.905	1.905	C7-C6-C1-N1	174.6 (3)	1.320	-0.242
C12-O2	1.355 (3)	1.350	1.349	N1-C8-C9	123.1 (3)	122.084	121.916
C1-N1-C8	119.89	121.088	128.618				

**Figure 3.** Superimposition of the X-ray structure (red) and calculated structure (black) of the title molecule for enol-keto tautomerism.

the molecular chemical stability (Shankar Rao et al 2006). The frontier orbital gap helps identify the chemical reactivity and kinetic stability of the molecule. The calculated energy values for enol-imine and keto-amine forms in gas phase are; $E_{\text{HOMO}}(\text{enol}) = -5.647$ eV, $E_{\text{LUMO}}(\text{enol}) = -1.672$ eV, $\Delta E(\text{enol}) = 3.975$ eV and $E_{\text{HOMO}}(\text{keto}) = -5.327$ eV, $E_{\text{LUMO}}(\text{keto}) = -1.988$ eV, $\Delta E(\text{keto}) = 3.338$ eV. By using

**Figure 4.** Total electron density mapped with molecular electrostatic potential surface.

HOMO and LUMO energy values for a molecule, the global chemical reactivity descriptors of molecules such as hardness, chemical potential, softness, electronegativity and electrophilicity index as well as local reactivity have been defined (Chattaraj et al 2003). The ionization energy (I) and electron affinity (A) can be obtained as, $I = -E_{\text{HOMO}}$ and $A = -E_{\text{LUMO}}$. Mulliken electronegativity (χ) can be calculated as follows: $\chi = (I + A)/2$. Softness (S) is a property of molecule that measures the extent of chemical reactivity. It is the reciprocal of hardness $S = 1/2\eta$. It is defined as the reciprocal of hardness (η) and $\eta = (I - A)/2$ (Chermette 1999). In addition, electrophilicity index (ω), $\omega = (-\chi^2/2\eta)$ as a measure of energy lowering due to maximal electron flow between donor and acceptor. The values of electronegativity, chemical hardness, softness, and electrophilicity index for enol and keto forms are 3.659 eV, 1.985 eV, 0.251 eV, -3.372 eV and 3.657 eV, 1.669 eV, 0.299 eV and -4.006 eV in gas phase, respectively. Lower values of softness and electrophilicity index is supported that enol form is more stable and more lower chemical activity.

3.3. Analysis of Molecular Electrostatic Potential (MEP) Surface

Molecular electrostatic potential (MEP) at a point in space around a molecule gives information about the net electrostatic effect produced at that point by total charge distribution (electron+proton) of the molecule and correlates with dipole moments, electro-negativity, partial charges and chemical reactivity of the molecules. The different values of the electrostatic potential at the surface are represented by different colors; red represents regions of most electronegative electrostatic potential, blue represents regions of the most positive electrostatic potential and green represents regions of zero potential. According to MEP map results, the negative regions are located on donor oxygen atom, acceptor nitrogen atom (red coded region). Besides, the positive regions (blue encoded regions) are located on methoxy group and concentrated on the hydrogen atoms around. The resulting surface simultaneously displays molecular size and shape and electrostatic potential value. As we seen from the MEP map, while regions having the negative potential are over the electronegative atoms (intensively, O1, N1, Br and O2 atom) because of the strong intra molecular hydrogen bonding and high electronegativity of Br atom. However only net negative region is shown on O1 atom because high positive atoms are curtailed the other electronegative atoms. As can be seen in MEP, deepest red on O1 and O2 atoms are a strongest attraction. The positive regions over the hydrogen atoms of O-CH₃ and all other hydrogen atoms are the most effective in nucleophilic processes. However, the H1 atom which is provding the proton transfer in the 6-membered ring has higher values than on the all other H atoms (Fig.4). The MEP surface provides necessary information about the reactive sites.

3.4. Mulliken Population Analysis and Natural Populatin Analysis (NPA)

The total atomic charge values are obtained by Mulliken population analysis by optimized geometry and Natural population charges are obtained by natural bond orbital analysis (NBO). All of the hydrogen atoms have net positive charges. The positive atomic charges show that the C12>H1>C14>C8>H7c>H7b>H15c>H15b>H15a>H7a>H8>H10>C9>H13>H3>H4>H5 and H1>C14>C12>H13>H10>H3>H4>H7b>H7a>H5>H15A>H7c>H8>H2>H15c>H15b>Br>C1>C8>C6 for Mulliken charges and Natural charges (NPA) results, respectively. This is due to the presence strong intramolecular hydrogen bond and steric interactions. The most negative atomic charges

are N1>O2>O1>C7=C1>Br>C5>C10>C13>C3>C6>C2>C15>C4>C11 and C7>O1>N1>O2>C13>C15>C2>C5>C3>C10>C11>C9>C4>C7 for Mulliken charges and Natural Charges (NPA) results, respectively. The results indicated that a little differences in Natural charges and Mulliken charges. The intention is to accurately model partial charge magnitude and location within a molecule. Mulliken population analysis is a good way to account for differences in electronegativities of atoms within the molecule and frequently uses for supporting the MEP. The results of MEP, NPA and mulliken population analyses could be use for interpreting and predicting the reactive behavior of a wide variety of chemical systems in both electrophilic and nucleophilic reactions.

3.5. Nonlinear Optical Properties (NLO)

Organic molecules able to manipulate photonic signals efficiently are of importance in technologies such as optical communication, optical computing, and dynamic image processing (Eaton 1991).

The calculated values of electronic dipole moment (μ), polarizability (α) and the first hyperpolarizability (β) for the titled molecule are 1.0597 Debye, 32.527 Å³ and 1.22× 10⁻²⁹ cm⁻⁵/esu. Urea is one of the prototypical molecules used in the study of the NLO properties of molecular systems. In NLO studies, the urea is used as reference and its calculated α and β values at B3LYP/6-31G(d,p) level were found as 3.8312 Å³ and 0.37289×10⁻³⁰ cm⁻⁵/esu, respectively (Sun et al 2009). Therefore the polarizability and hyperpolarizability of the title molecule is approximately 8.5 and 32.8 times greater than those of urea. It is well known that if the molecule has many delocalization π electrons, bigger change of dipole moment from ground state to excited state, large transition moment and noncentrosymmetry structure, the molecule will have strong second order NLO response (Yıldırım et al 2005). According to the magnitude of the first hyperpolarizability and extended π -electron delocalization in the system, the title compound may be a potential applicant in the development of NLO materials.

3.6. Fukui Function Analysis

The Fukui function is among the most basic and commonly used reactivity indicators. The Fukui function is given as the change in the density function $\rho(r)$ of the molecule as a consequence of changing the number of electrons N in the molecule, under the constraint of a constant external potential. The Fukui function is defined as:

Table 4. Values of the fukui function considering Natural population analysis (NPA).

Atom	f ⁻	f ⁺	f ⁰	Atom	f ⁻	f ⁺	f ⁰
C1	0.091	0.112	0.072	O2	-0.252	-0.192	-0.250
C2	-0.112	-0.090	-0.127	Br	-0.002	0.149	0.034
C3	-0.136	-0.1114	-0.118	H1	0.256	0.262	0.260
C4	-0.104	-0.004	-0.118	H2	0.113	0.126	0.119
C5	-0.131	-0.135	-0.118	H3	0.107	0.133	0.120
C6	-0.003	0.060	-0.012	H4	0.104	0.131	0.120
C7	-0.344	-0.3584	-0.350	H5	0.106	0.132	0.118
C8	0.142	0.023	0.062	H7A	0.107	0.131	0.120
C9	-0.110	0.031	-0.103	H7B	0.122	0.134	0.125
C10	-0.048	-0.143	-0.097	H7C	0.121	0.132	0.124
C11	-0.122	0.028	-0.091	H8	0.079	0.116	0.102
C12	0.212	0.218	0.172	H10	0.114	0.141	0.128
C13	-0.214	-0.196	-0.186	H13	0.116	0.142	0.129
C14	0.230	0.256	0.202	H15A	0.107	0.130	0.119
C15	-0.160	-0.172	-0.165	H15B	0.100	0.116	0.106
N1	-0.234	-0.149	-0.263	H15C	0.100	0.116	0.106
O1	-0.354	-0.272	-0.346				

Table 5. Second-order perturbation theory analysis of Fock matrix in NBO basis for the title compound.

Donor(i) (occupancy)	Type	ED _A , % ED _B , %	Acceptor(j) (occupancy)	Type	ED _A , % ED _B , %	E ^{(2)a} (kcal/mol)	E _j -E _i ^b (a.u.)	F(ij) ^c (a.u.)
BD C2-C3 (1.97817)	σ	49.58 50.42	BD*C1-N1 (0.02789)	σ*	60.21 39.79	4.04	1.14	0.061
BD C1-C2 (1.65075)	π	50.35 49.65	BD*C3-C4 (0.34036)	π*	50.0 50.0	20.36	0.29	0.068
BD C1-C2 (1.65075)	π	50.35 49.65	BD*C8-N1 (0.22294)	π*	62.20 37.80	9.04	0.26	0.045
BD C8-N1 (1.91597)	π	37.80 62.20	BD*C1-C2 (0.38474)	π*	49.65 50.35	9.99	0.37	0.059
BD C8-N1 (1.91597)	π	37.80 62.20	BD*C9-C10 (0.45617)	π*	43.10 56.90	7.31	0.36	0.050
BD C9-C10 (1.63899)	π	56.90 43.10	BD*C8-N1 (0.22294)	π*	62.20 37.80	25.81	0.26	0.076
BD C11-C12 (1.60662)	π	59.11 40.89	BD*C9-C10 (0.45617)	π*	43.10 56.90	28.19	0.29	0.082
BD C12-C13 (1.97234)	σ	50.43 49.57	BD*C11-Br (0.02826)	σ*	50.34 49.66	4.06	0.82	0.051
BD O1-H1 (1.98459)	σ	79.47 20.53	BD*C1-N1 (0.02789)	σ*	60.21 39.79	0.68	1.18	0.025
BD O1-H1 (1.98459)	σ	79.47 20.53	BD*C13-C14 (0.02289)	σ*	49.86 50.14	5.72	1.29	0.077
LP N1 (1.83997)	n	-	BD*O1-H1 (0.08221)	σ*	20.53 79.47	32.68	0.78	0.146
BD*C1-C2 (0.38474)	π*	49.65 50.35	BD* C5-C6 (0.32778)	π*	50.72 49.28	288.98	0.01	0.082

^a E⁽²⁾ means energy of hyperconjugative interactions (stabilization energy). ^b Energy difference between donor (i) and acceptor (j) NBO orbitals. ^c F(i,j) is the Fock matrix element between i and j NBO orbital. Percentage electron density over bonded atoms (ED_{A/B}, %).

$$F(r) = \frac{\partial \rho(r)}{\partial N} r \quad (1)$$

where $\rho(r)$ is the electronic density, N is the number of electrons and r is the external potential exerted by the nuclease. Fukui functions are introduced, which are advocated as reactivity descriptors in order to identify the most reactive sites for electrophilic or nucleophilic reactions within a molecule. The Fukui function indicates the propensity of the electronic density to deform at a given position upon accepting or donating electrons (Parr and Yang 1989). Also, it is possible to define the corresponding condensed or atomic Fukui functions on the j_{th} atom site as,

$$f_j^- = q_j(N) - q_j(N-1) \quad (2)$$

$$f_j^+ = q_j(N+1) - q_j(N) \quad (3)$$

$$f_j^0 = \frac{1}{2}[q_j(N+1) - q_j(N-1)] \quad (4)$$

for an electrophilic $f_j^-(r)$, nucleophilic or free radical attack $f_j^+(r)$ on the reference molecule, respectively. In these equations, q_j is the atomic charge (evaluated from Mulliken population analysis, electrostatic derived charge, etc.) at the j th atomic site in the neutral (N), anionic ($N+1$) or cationic ($N-1$) chemical species (Ayers and Parr 2000).

The values of the Fukui function calculated from the NBO charges. From Table 6, note the presence of negative values of the Fukui function. Recently it was reported that a negative Fukui function value means that when adding an electron to the molecule, in some spots, the electron density is reduced; alternatively when removing an electron from the molecule, in some spots, the electron density is increased.

From the calculated values, the reactivity order for the electrophilic case was $O1 > C7 > O2 > N1 > C13 > C15 > C8 > C3 > C5 > C9 > C4 > C10 > C6 > Br$. On the other hand, for nucleophilic attack we can observe $H1 > C14 > C12 > H13 > H10 > Br > H-7B > H3 > H7C > H5 > H7A > H4 > H15A > H2 > H8 > H15C > H-15B > C1 > C6 > C9 > C8 > C11$. Position of reactive electrophilic sites and nucleophilic sites are accordance with the total electron density surface and chemical behavior. If one compares the three kinds of attacks it is possible to observe that, electrophilic attack is bigger reactivity comparison with the nucleophilic and radical attack.

3.7. Donor Acceptor Interactions: Natural Bond Orbital Analysis (NBO)

NBO method represents information about interactions in filled and virtual orbital spaces that could improve the analysis of intra and intermolecular interactions. It also

provides a convenient basis for investigating charge transfer or conjugative interaction in molecular systems. The larger energy of hyperconjugative interactions $E^{(2)}$ value, the more intensive is the interaction between electron donors (i) and electron acceptors (j).

The structure is a type of total Lewis structure with % 97.79 (core, % 99.97; valance Lewis, % 96.37) and total non Lewis with % 2.2 (Rydberg non-Lewis, % 0.13; valance non-Lewis, %2.06).

The interactions $\pi(C-C)$ and their antibonding π^* interactions are responsible for conjugation of respective π -bonds in benzene rings. The electron density at the conjugated π bonds (1.60-1.91) of benzene rings and π^* bonds (0.22-0.49) of benzene rings indicate strong π -electron delocalization within ring leading to a maximum stabilization of energy ~ 31 kcal/mol. The charge transfer interactions are formed by the orbital overlap between bonding (π) and antibonding (π^*) orbitals, which results in intramolecular charge transfer (ICT) causing stabilization of the system. The movement of π -electron cloud from donor to acceptor i.e. ICT can make the molecule more polarized and it must be responsible for the NLO properties of molecule (Sylvestre et al 2014). Therefore, the titled molecule can be ideal material for non-linear optical applications in future. The interactions of single-double bond arrangement which are leads to enol-keto tautomerism are chemically significant and they could be used as a measure of the intramolecular delocalization, hyperconjugative interactions of the $E^{(2)}$ values. the higher stabilization of $E^{(2)}$ energy is related to the resonance in benzene rings and double bond steric interactivity. The $\pi^* \rightarrow \pi^*$ and $n \rightarrow \pi^*$ interactions show high $E^{(2)}$ energy because of crystal packing, electron absorption and charge transfer interactions. The strong stabilization energies of $n(O1) \rightarrow \pi^*(C13-C14)$, $\pi^*(C1-C2) \rightarrow \pi^*(C5-C6)$, $\pi^*(C11-C12) \rightarrow \pi^*(C9-C10)$, $\pi^*(C11-C12) \rightarrow \pi^*(C13-C14)$, are 40.59 kcal/mol, 288.98 kcal/mol, 199.1 kcal/mol, 191.981 kcal/mol, respectively (Table 5).

4. Discussion and Conclusion

To support the experimental results, the geometric parameters were calculated by using the DFT method and compared with the X-ray results. The theoretically calculated values of both geometric parameters of the structure of the minimum energy were investigated and then, enol-keto tautomers were compared with X-ray crystallographic data. The theoretical results of the geometric parameters are successfully represented experimental data. X-ray

investigation shows that the titled compound exists in enol form in the solid state. The values of electronegativity, chemical hardness, softness, and electrophilicity index have been calculated and the results show that enol-imin form is more stable than keto-amine form. According to stability of the molecule to softness means that the molecule with least HOMO–LUMO gap and it means that it is more reactive molecule. Fukui function analysis helps to identifying the electrophilic and nucleophilic nature of a specific site within a molecule. MEP, Mulliken population analysis, NPA results are consistent with each other related to chemically reactivities of molecule. Natural bond orbital (NBO) calculations reveal the delocalization and hyperconjugation interaction, intramolecular charge transfer and stabilization energy of molecule. According to NBO results, we can determine the ideal Lewis type structure. This ideality has also been arised percentage of valence hybrids of the atoms and the weight of each atom in each localized electron pair bond, clearly. Low HOMO–LUMO energy gap and high partial positive regions support the molecule for high first hyperpolarizability value, so its make the strong optical material applicant. We hope the results of this study will help researchers to design and synthesis new metal materials.

5. References

- Ayers, PW., Parr, RG. 2000.** Variational principles for describing chemical reactions: the fukui function and chemical hardness revisited. *J. Am. Chem. Soc.*, 122(9): 2010–2018.
- Boyle, NMO., Tenderholt, AL., Langer, KM. 2008.** cclib: a library for package-independent computational chemistry algorithms. *J. Comp. Chem.*, 29: 839–845.
- Chattaraj, PK., Maiti, B., Sarkar, U. 2003.** Philicity: a unified treatment of chemical reactivity and selectivity. *J. Phys. Chem.*, A107: 4973–4975.
- Chermette, H. 1999.** Chemical reactivity indexes in density functional theory. *J. Comp. Chem.*, 20: 129–154.
- Dhar, DN., Taploo, CL. 1982.** Schiff bases and their applications. *J. Sci. Ind. Res.*, 41(8): 501–506.
- Eaton, DF. 1991.** Nonlinear optical materials. *Sc.*, 253: 281–287.
- Etter, MC. 1990.** Encoding and decoding hydrogen-bond patterns of organic compounds. *Acc. Chem. Res.*, 23(4): 120–126.
- Gaussian, RA., Frisch, MJ., Trucks, GW., Schlegel, HB., Scuseria, GE., Robb, MA., Cheeseman, JR., Scalmani, G., Barone, V., Mennucci, B., Petersson, GA. 2009.** Gaussian. *Inc., Wallingford CT.*
- Murray, JS., Sen, K., 1996.** Molecular Electrostatic Potentials, Concepts and Applications, Elsevier, Amsterdam, pp 664.
- Özek, A., Albayrak, Ç., Odabasoğlu, M., Büyükgüngör, O. 2007.** Three (E)-2-[(bromophenyl)iminomethyl]-4-methoxyphenols. *Acta Crystallogr. C*, 63: o177.
- Parr, RG., Yang, W. 1989.** Functional Theory of Atoms and Molecules, Oxford University Press, New York, pp 333.
- Shankar Rao, YB., Prasad, MVS., Udaya Sri, N., Veeraiyah V. 2006.** Vibrational (FT-IR, FT-Raman) and UV-Visible spectroscopic studies, HOMO–LUMO, NBO, NLO and MEP analysis of Benzyl (imino (1H-pyrazol-1-yl) methyl) carbamate using DFT calculations. *J. Mol. Struct.*, 1108: 567–582.
- Sheldrick, GM. 2008.** A short history of SHELX. *Acta Cryst. A: Found. Cryst.*, 64(1): 112–122.
- Stoe, C. 2002.** X-area (version 1.18) and X-red32 (version 1.04). *Stoe & Cie, Darmstadt, Germany.*
- Sun, YX., Hao, QL., Wei, WX., Yu, Z.X., Lu, L.D., Wang, YS. 2009.** Experimental and density functional studies on 4-(3, 4-dihydroxybenzylideneamino) antipyrine, and 4-(2, 3, 4-trihydroxybenzylideneamino) antipyrine. *J. Mol. Struct.*, 904: 74–82.
- Sylvestre, S., Sebastian, S. Edwin, S., Amalanathan, M., Ayyapan, S., Jayavarthanam, T., Oudayakumar, K., Solomon, S. 2014.** Vibrational spectra (FT-IR and FT-Raman), molecular structure, natural bond orbital, and TD-DFT analysis of L-Asparagine Monohydrate by Density Functional Theory approach. *Spect. Acta Part A: Mol. and Biom. Spect.*, 133: 190–200.
- Yıldırım, MH., Pasaoğlu, H., Odabasoğlu, HY., Odabasoğlu, M., Özek Yıldırım, A., 2015.** Synthesis, structural and computational characterization of 2-amino-3,5-diiodobenzoic acid and 2-amino-3,5-dibromobenzoic acid. *Spect. Acta Part A: Mol. and Biom. Spect.*, 146: 50–60.